

Effects of particle size of crushed gangue backfill materials on surface subsidence and its application under buildings

Meng Li¹ · Jixiong Zhang¹ · Yanli Huang¹ · Nan Zhou¹

Received: 5 August 2016 / Accepted: 18 August 2017 / Published online: 30 August 2017
© Springer-Verlag GmbH Germany 2017

Abstract In recent years, solid waste backfill mining has developed rapidly and widely used to control surface subsidence and reduce accumulation of solid waste. As crushed materials are used to backfill goafs, the particle size of backfill materials becomes a key factor influencing the control of surface subsidence. To analyse the influences of particle size of backfill materials on surface subsidence, the compaction properties of crushed gangue backfill materials (CGBM) with different particle sizes were tested by using the YAS5000 testing machine and a self-made compacting device. Moreover, based on the strain hardening behaviour of CGBM in the process of compaction, a method of simulating CGBM using double-yield model was put forward. By employing this method in simulation, the influence of particle size of CGBM on surface subsidence was studied. The research results are demonstrated as follows: with the increase in particle size of the backfill materials, these maximum values such as the maximum surface subsidence, horizontal movement, inclination, curvature, and horizontal deformation increased gradually. Little difference was found in the surface subsidence and movement while using CGBM with particle sizes in the ranges of 2.5–16 and 2.5–50 mm with uniform gradation. However, both values were obviously smaller than those using CGBM with particle sizes of 20–31.5 and 31.5–50 mm. In terms of samples with particle sizes of 2.5–50 mm, the gradation of particles was uniform. By using large particles to form frame structures and small

particles to fill fractures, such structures with strong anti-deformation abilities produced a small amount of deformation under the load from overlying strata. Therefore, this structure exerted a good controlling effect on surface deformation.

Keywords Crushed gangue · Backfill materials · Surface subsidence · Particle size · Under buildings

Introduction

In China, as the coal mine goaf is usually not to be back-filled, sudden, significant strata movement and large-scale surface subsidence are inevitable (Unver and Yasitli 2006; Wang et al. 2008; Cui et al. 2014), which results in various problems such as damage to buildings, village relocation, depletion of water resources, and land desertification (Loupasakis et al. 2014; Oparin et al. 2014; Guo et al. 2017). Statistics indicates that the subsiding areas induced by caving coal mining annually amount to about 40,000 hm² and the financial losses caused are about 2 billion RMB every year. At present, in China, the total area of coal mining-induced surface subsidence has reached 700,000 hm². Additionally, the unexploited coal under buildings, under railways, and under water bodies amounts to 13.79 billion tons, among which the unexploited coal beneath buildings accounts for about 9.468 billion tons, making up 69% of all unexploited coal and involving 2030 villages in mining areas (Zhang et al. 2011; Li et al. 2014). Furthermore, in the process of coal mining, a large amount of solid waste is produced and accumulated on the ground, taking up significant land resources and polluting the environment (Brake et al. 2001; Skierszkan et al. 2016). In recent years, with the intensification and deepening of coal

✉ Jixiong Zhang
zjxiong@cumt.edu.cn

¹ Key Laboratory of Deep Coal Resource Mining, School of Mines, Ministry of Education of China, China University of Mining and Technology, Xuzhou 221116, China

mining works, consequent environment problems (Jirina and Jan 2010; Fan et al. 2014) have become increasingly serious including surface subsidence and the accumulation of solid waste, especially for those mines with significant amounts of the aforementioned coal mining issues. Therefore, it has become a research focus for those seeking to develop an effective technique for controlling surface subsidence while simultaneously disposing of the resulting solid waste. Under this background, some techniques such as paste backfill (Belem and Benzaazoua 2008; Orejarena and Fall 2010), grout injection into the overburden (Palarski 1989; Xuan and Xu 2014; Xuan et al. 2016), and solid waste backfill mining (SWBM; Junker and Witthaus 2013; Zhang et al. 2014) have been proposed to solve the aforementioned problems.

Because of its low costs and good backfill effects, the SWBM technique has been developed rapidly and it has been more widely used in recent years. This technology is developed based on fully mechanised coal mining. Solid wastes are transported into shafts using a vertical feeding system (Zhang et al. 2017), and then, the crushed wastes in the shafts are directly poured into goafs on backfill panels to support the overlying strata on a permanent basis. In this way, the strata movement and surface subsidence are better controlled: because granular materials are used as backfill materials in this technology, the rules governing surface subsidence are completely different from those governing paste backfill (Guo et al. 2014). Moreover, the particle size of backfill materials, as a key factor, affects the surface subsidence. Pouring backfill materials with different particle sizes into goafs can result in different controlling effects being exerted on surface subsidence. Therefore, the influence of particle size of backfill materials on surface subsidence needs to be investigated.

The 13,080 backfill panel in the No. 12 coal mine of the Pingmei Group (Pingdingshan, China) was investigated. As there is a high density of surface buildings on this backfill panel and a lot of gangues were stockpiled on the ground, the SWBM technique was adopted to solve these problems. In this research, by testing the compaction properties of crushed gangue backfill materials (CGBM) with different particle sizes, a method of simulating of CGBM was proposed to study the influences of particle sizes of CGBM on surface subsidence.

Study site

The No. 12 coal mine, Pingmei Group, which is located in Pingdingshan mining area, China, was selected as a case study. As the coal resources in the coal mines are exploited gradually, a large amount of coal resources has been found beneath the village and its buildings. Thus, those buildings

overlying the coal reserves have been affected adversely by the mining activity of the No. 12 coal mine. Meanwhile, around 8 million tons of gangues is produced every year, which are stockpiled on the ground surface. To solve the aforementioned problems, the SWBM technique was adopted during mining to protect these buildings from the influence of coal mining. The SWBM technique was first applied to the 13,080 longwall mining panel, where the recoverable reserves amounted to 124,000 tons. This panel is overlain by three villages, and the corresponding buildings are mainly masonry structures (Fig. 1). Given the mining regulations for exploiting the coal under buildings and the density of buildings above the panels, the maximum fortification indices for the displacement and deformation of the ground were determined. Hence, the maximum subsidence is expected to be smaller than 500 mm, and the maximum values of horizontal compressive and stretching deformations need to be larger than -2 mm/m and smaller than 1.5 mm/m, respectively. Additionally, the maximum curvature and inclination are supposed to be smaller than 0.2 and 2 mm/m, respectively.

The layout of the 13,120 backfill panel is shown in Fig. 1. The panel has an overburden depth of 360 m and is 350 m long in the strike direction and 100 m wide in the dip direction. The mining seam is about 3.3 m thick. The geological core log of the surrounding rocks indicates that the immediate roof of the panel is shale with an average thickness of 5.3 m, the main roof is sandstone with an average thickness of 31.5 m and the immediate floor of the panel is mudstone with an average thickness of 15.9 m. To protect the environment, and dispose of the gangues in the meantime, they were crushed to serve as backfill materials in the 13,080 backfill panel.

Effect of CGBM on surface subsidence

The SWBM technique, developed from fully mechanised coal mining methods, can realise coal mining and backfill at the same time under the cover of a backfill support. Compared with fully mechanised coal mining, SWBM has the same coal mining system but uses a vertical feeding system which can safely and efficiently convey solid waste to the goaf in the panel and a compaction system behind the backfill support, as illustrated in Fig. 2.

The fundamental principle of the SWBM technique is used to convey solid waste such as gangues, construction waste, coal ash, and mineral waste residues to a storage bin in the shaft by using a vertical feeding system. Then, using an underground transportation system, the backfill materials in the storage bin are transported to a backfill conveyor hanging in the back top beam of the backfill support (Fig. 3a). Afterwards, the backfill materials are poured into

Fig. 1 Distribution of surface buildings and layout of the 13,080 backfill panel

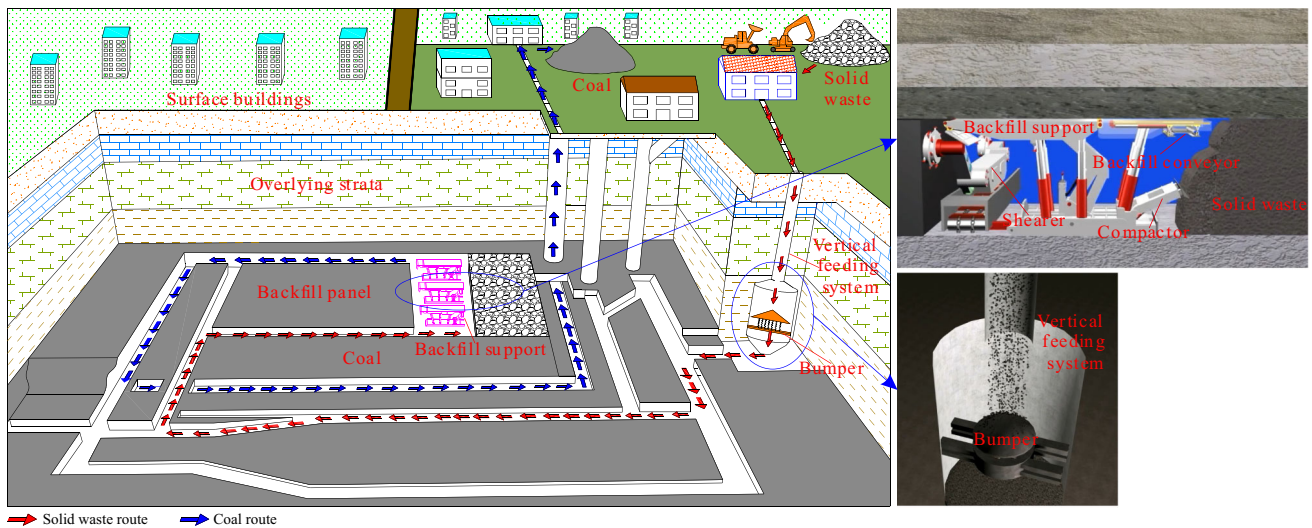
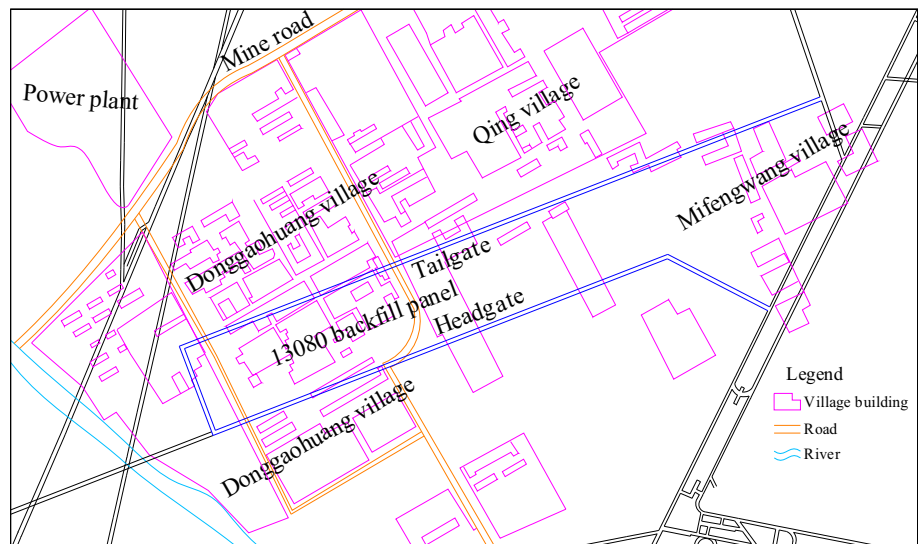


Fig. 2 Fundamental principle of the SWBM technique

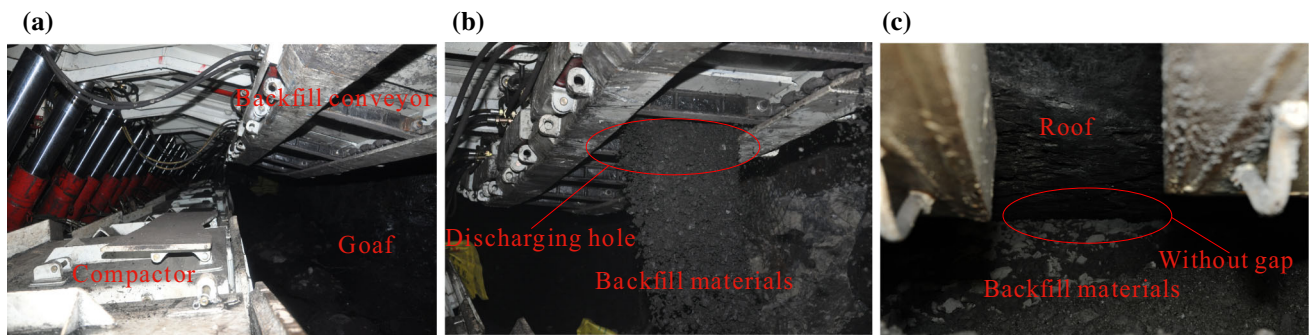


Fig. 3 Photograph of underground backfill conditions. **a** Backfill support, **b** backfill conveyor, **c** no gap with roof

the goaf through a discharging hole in the backfill conveyor (Fig. 3b) and then compacted by a compactor until they make contact with the roof, leaving no gap (Fig. 3c).

For traditional fully mechanised coal mining, with the advance of the panel, the roof caves and breaks under the load of the overlying rock strata, and then, the caving and

breakage extend to the overlying strata, generating caving, fracture, and bending zones, which form a large-scale subsidence basin (Fig. 4a), while in SWBM, as the working face was advanced, backfill materials filled the goaf and then made contact with the roof. In this case, the overlying strata mainly bent and subsided with fractures only appearing in local areas and no caving zone is found, which validates the idea that the SWBM technique is effective in controlling surface subsidence (Fig. 4b).

According to rules of coal mining-induced surface subsidence, the surface subsidence after mining coal seams is directly related to mining height. The smaller the mining height, the smaller the surface subsidence, and vice versa. When the backfill materials are backfilled into goafs, it means that the mining height has decreased. As a result, under the load from the overlying strata, the stiffer the backfill material, the lower the deformation. This results in a good controlling effect being exerted upon the surface subsidence.

Compaction properties of CGBM

Sample preparation

The samples used for testing compaction properties were taken from the gangue hills in the No. 12 coal mine of the Pingmei Group. The gangues were sandy mudstones and the samples were prepared in the laboratory. First of all, the sandy mudstones were crushed into particles with a diameter of less than 50 mm by using steel hammers. Afterwards, according to the particle size, the crushed sandy mudstones were sieved stepwise to those with particle sizes of 2.5, 10, 16, 20, 31.5, and 40 mm using standard stone screens.

To investigate the influences of particle size on compaction properties of samples, the prepared samples were

classified into four groups A (2.5–16 mm), B (20–31.5 mm), C (31.5–50 mm), and D (2.5–50 mm) according to the particle size.

Experimental apparatus

As shown in Fig. 5, the experimental system mainly consists of a YAS5000 electro-hydraulic servo testing machine and a self-made compaction device. The maximum axial force provided by the test machine was 5000 kN. Equipped with data acquisition software, the system can obtain the mechanical parameters such as load and displacement. The compaction device comprised a steel chamber, a base, a dowel bar, and a loading plate. The internal radius, external radius, height, and wall thickness of the steel chamber were 125, 137, 305, and 12 mm, respectively. The steel chamber and base were connected by flanges. In addition, with a radius and a height of 124 and 40 mm, respectively, the loading plate was able to apply a uniform force to the samples. Meanwhile, a strain gauge was used to monitor the strain in the chamber walls during compaction.

Experiment methods and procedures

During compaction, lubricating greases were smeared over the inner wall of the chamber to reduce the friction between the chamber wall and the samples. Meanwhile, four pairs of strain gauges were arranged on the outer wall of the chamber to monitor the strains in the chamber walls, so as to inversely compute the friction forces thereon. Then, the pressure on the samples was obtained by subtracting the friction forces from the total pressure produced by the testing machine.

In the compaction process, Δh represents the compaction deformation of samples and h_0 indicates the height of samples before compaction. The strain in a sample is defined as:

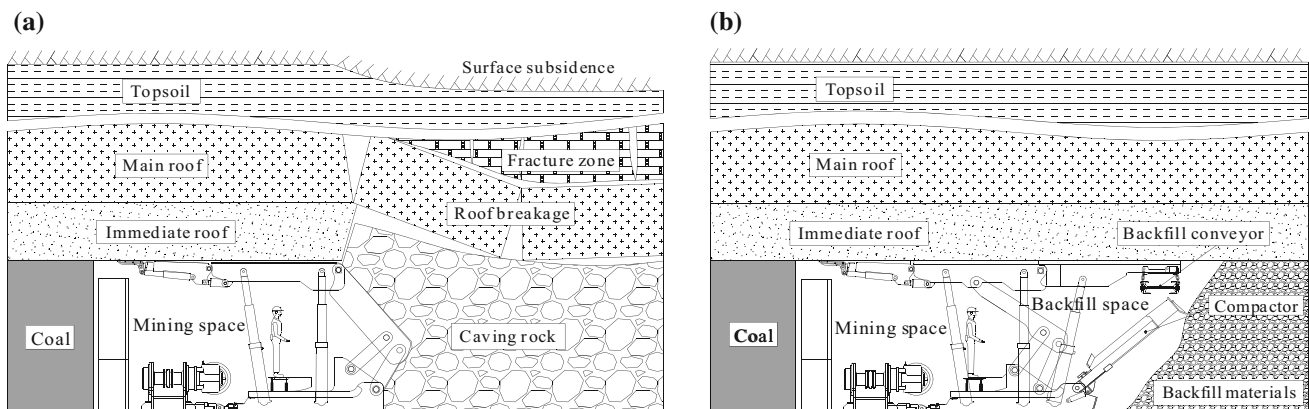


Fig. 4 Characteristics of strata movement. **a** Caving mining, **b** SWBM

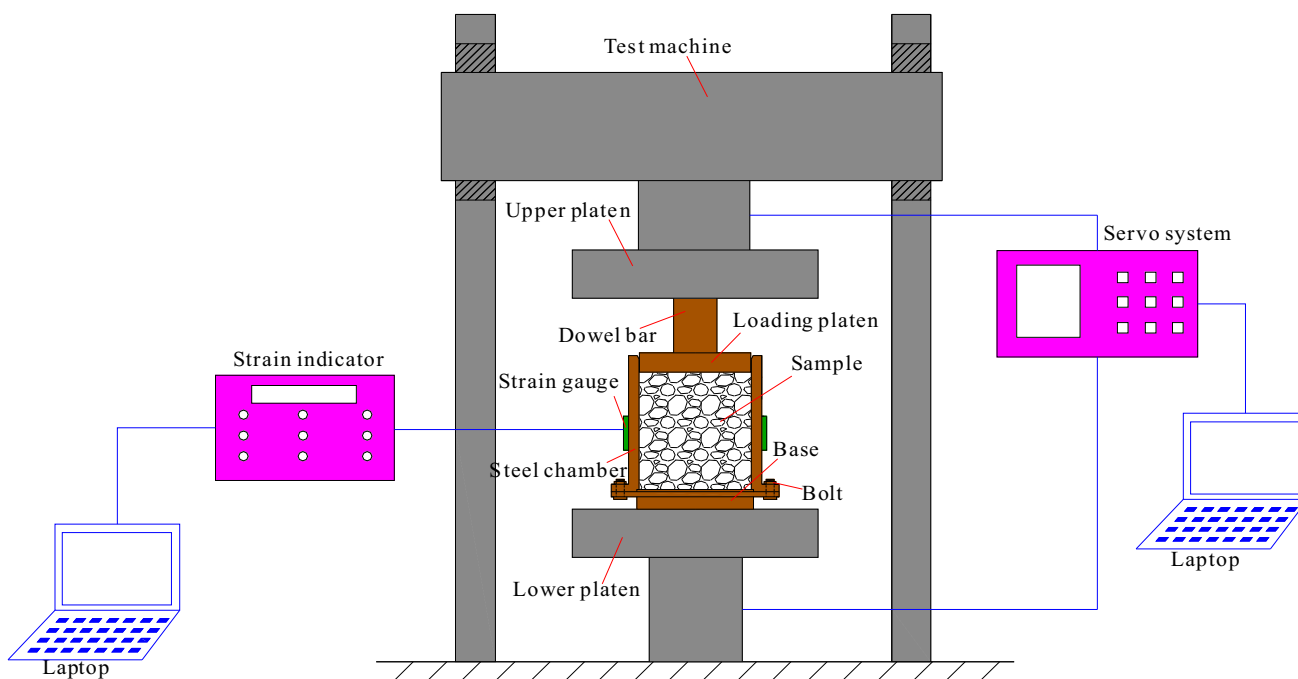


Fig. 5 Experimental system

$$\varepsilon = \frac{\Delta h}{h_0} \tag{1}$$

In Eq. (1), before compacting the samples, their initial height was calculated. When the samples were placed into the compaction device, according to the height h_1 of the steel chamber, the height h_2 of the dowel bar, the thickness h_3 of the loading plate, and the height h_4 of the dowel bar exceeding the steel chamber, the height of samples before being compacted was thus $h_0 = h_1 + h_4 - h_2 - h_3$. However, as shown in Fig. 6, h_1 , h_2 , and h_3 were given; thus, $h_0 = h_4 + 145$.

Specific experimental steps were as follows:

1. Samples were weighed and put into the compaction device. Samples of 9 kg were weighed for each group and then placed into a compaction device in several layers. Afterwards, the sample surface was struck off until smooth.
2. We calculated the height h_0 of samples before compaction. After the samples were put into the chamber, the loading plate was placed on the surface of samples so as to make contact with the samples, and then, the height of the sample before compaction was calculated.
3. We placed the compaction device into the testing machine to apply load to the samples.

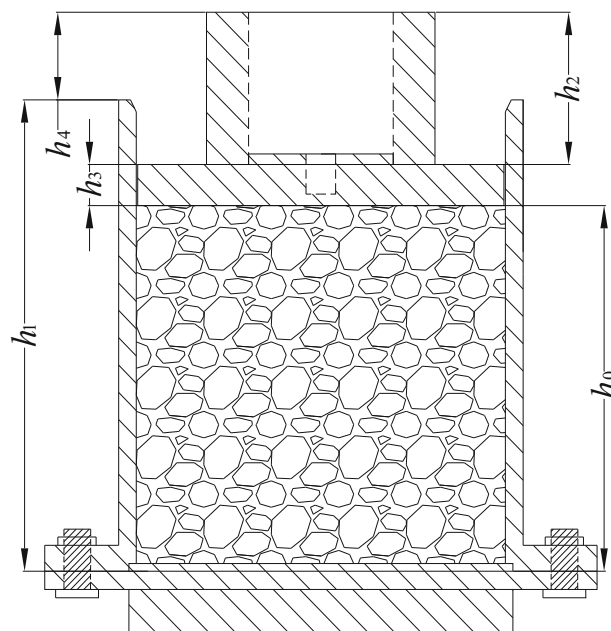


Fig. 6 Calculation of the sample height before compaction

Before loading, the positions of the top pressure plate and the dowel bar of the test machine were adjusted to align the dowel bar with the centre of the top pressure plate and let it make contact with the top pressure plate. Meanwhile, the displacement, load, and strain of the chamber walls were recorded during the compaction of the samples.

Experimental results

The stress–strain curves of samples with different particle sizes were obtained (Fig. 7). The stress–strain relationship of each group of samples showed nonlinear compaction and deformation properties. In addition, with increasing axial stress, the strain in the samples increased gradually, while the increasing amplitude was reduced and it was eventually stabilized. Thus, strain hardening (Pappas and Mark 1993) therefore could be deemed to have occurred.

As shown in Fig. 7, the whole compaction process was divided into three stages including rapid compaction, slow compaction, and stable compaction. In the first stage, due to the existence of large voids between particles, the samples presented a low stiffness, resulting in rapid deformation, while during the slow compaction stage, a large number of particles were crushed with the increasing strain; thus, the pores were filled with crushed small particles so as to reduce the porosity. In this way, the stiffness of the samples increased, leading to a decrease in the rate of increase in strain. Moreover, at the stage of stable compaction, the samples became well compacted.

With respect to the samples in group A, they had small particle sizes and few pores between particles as well as a high stiffness. With the growth in particle size, the samples were more deformed during compaction. However, the deformation of samples in group D was similar to group A. Such results were explained by considering that, as the frame structure was formed by the large particles, the small particles in group D samples filled the pores between the frame structures; thus, the stiffness increased.

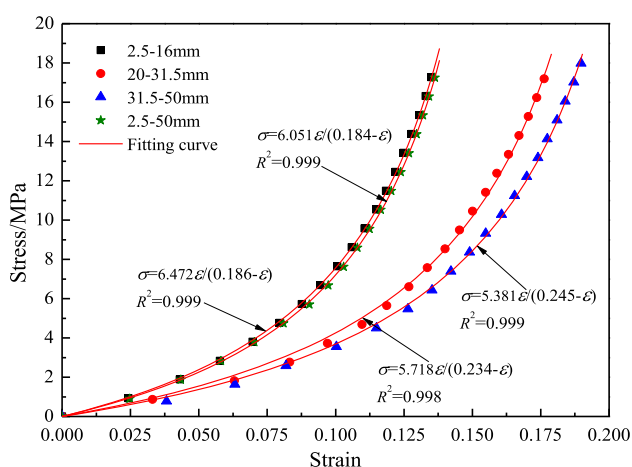


Fig. 7 Stress–strain curves of backfill materials with different particle sizes

Numerical simulation

CGBM simulation methods

When CGBM was poured into goafs, under the load imposed by the overlying strata, the backfill materials were gradually hardened through compaction and showed typical strain hardening behaviour. The double-yield (DY) model (Yavuz 2004) developed using FLAC^{3D} could be used to simulate this strain hardening, and this model was intended to represent a material in which there was significant irreversible compaction. Therefore, based on the compaction properties of CGBM, the double-yield model was used to simulate the compaction behaviour of backfill materials. The input parameters for the DY model can be divided into two parts: material properties and stress–strain data. Thereinto, the material properties included bulk modulus, shear modulus, friction angle, and dilation angle. The stress–strain data were obtained from the compaction trials (Fig. 7). To determine the properties of CGBM, a simple model was built which measured 1 m × 1 m × 1 m. A velocity was applied to the top of the model with confined sides to simulate the loading. The material properties were obtained by changing the bulk and shear modulus, friction angle, and dilation angle in the DY model iteratively to match the stress–strain curve to that found experimentally. Figure 8 shows the comparison of the stress–strain curves solved by numerical model and experimental data: they were well matched and the final properties of CGBM are listed in Table 1.

Establishment of the model and simulation program

The FLAC^{3D} software was used to build the numerical model based on the geological conditions of the 13,080

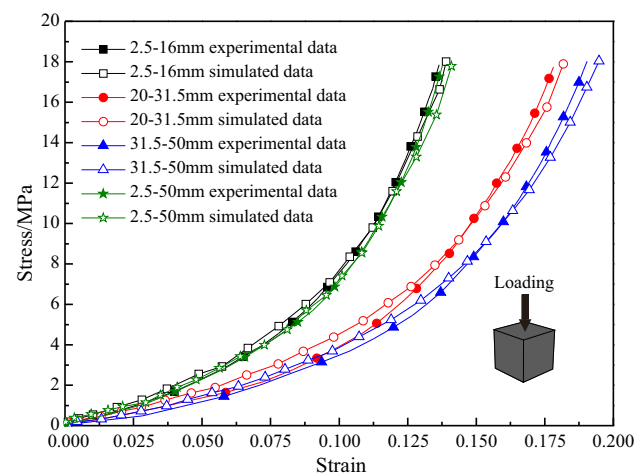


Fig. 8 Comparison of the stress–strain curves obtained by numerical models and experimental data

Table 1 Final mechanical properties of CGBM with different particle sizes

No.	Properties				
	Stress–strain data	Bulk modulus (MPa)	Shear modulus (MPa)	Dilation angle (°)	Friction angle (°)
A	$\sigma = 6.472\varepsilon/(0.186-\varepsilon)$	1933.08	11.62	5	28
B	$\sigma = 5.718\varepsilon/(0.234-\varepsilon)$	1357.54	8.16	6	30
C	$\sigma = 5.381\varepsilon/(0.245-\varepsilon)$	1220.17	7.33	8	32
D	$\sigma = 6.051\varepsilon/(0.184-\varepsilon)$	1826.67	10.98	5	29

backfill panel, as shown in Fig. 9. The dimensions of the model are 1350 m × 900 m × 375 m. The Mohr–Coulomb criterion was used to simulate the rock strata, and the DY model was adopted to simulate the CGBM, respectively. In total, the model is composed of 931,500 elements and 963,380 grid points. Due to computation time consumption and capacity restrictions, elements are fined in mining area with the size of 1.0 m. The rock strata properties used in this numerical model are summarised in Table 2: they have been scaled and adjusted following the work of Mohammad et al. (1997) and Xu (2001).

Four simulation programs were developed so as to investigate the effects of particle size of CGBM on surface subsidence. After the backfill panels were mined, the backfill materials, with their different mechanical parameters (Table 1), were adopted to backfill the goafs. In addition, the surface subsidence was simulated when the particle sizes were 2.5–16 mm, 20–31.5 mm, 31.5–50 mm, and 2.5–50 mm, respectively. The specific simulation steps are demonstrated in Fig. 10. Firstly, based on the constructed numerical model, the states of virgin stress in the

model that were not influenced by mining were simulated. Afterwards, the coal seams of the backfill panels were mined at a certain advance distance l_a (for example, 5 m) and the model was run through 50 iterations. Finally, by using the DY model to backfill the mining areas, the calculation was continued until the model reached equilibrium. The above steps were repeated until the whole backfill panel was excavated and filled.

Model verification

To verify the feasibility of the model, the simulation results were compared with the measured in situ results. In practical application, backfill materials graded to 2.5–50 mm were poured into the 13,080 backfill panel, so the mechanical parameters of samples in group D in Table 1 were adopted to simulate the backfill materials. When mining and filling the backfill panel, the internal stress of the backfill materials and the roof subsidence were monitored, as shown in Fig. 11. The instrumentation measuring the stress and the roof subsidence was fixed in the centre of

Fig. 9 Numerical simulation model

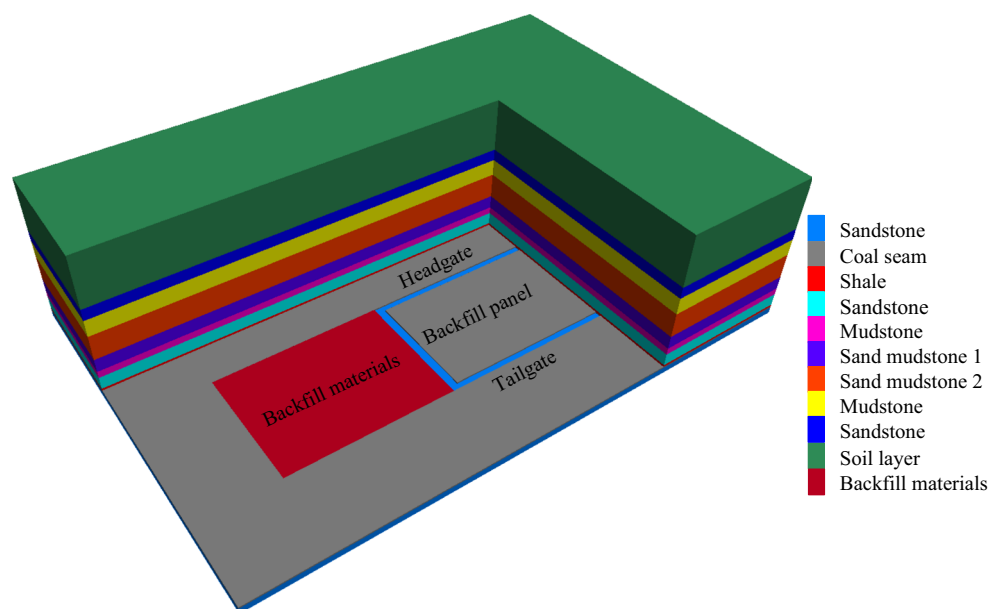
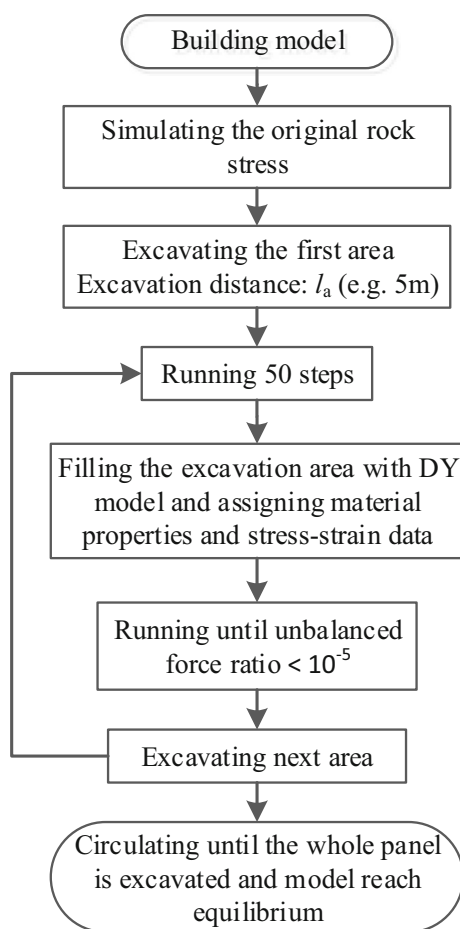


Table 2 Rock strata properties used in the numerical model

Rock strata	Bulk modulus (GPa)	Shear modulus (GPa)	Tensile strength (MPa)	Cohesion (MPa)	Friction angle (°)
Soil layer	0.25	0.1	0.001	0.02	22
Sandstone	11.3	8.4	1.8	3.3	35
Mudstone	5.6	3.8	0.8	1.9	26
Sand mudstone 1	7.3	5.2	1.1	2.2	28
Sand mudstone 2	7.5	5.4	1.2	2.3	30
Mudstone	5.3	3.6	0.8	1.8	25
Sandstone	10.8	8.1	1.6	3.1	33
Shale	8.5	6.4	1.4	2.6	31
Coal seam	2.8	1.5	0.4	0.9	20
Sandstone	11.2	8.3	1.5	3.2	34

**Fig. 10** Specific simulation steps

the backfill panel and 40 m away from the position of the open-off cut to monitor the internal stress on the backfill materials and the roof subsidence dynamically. Figure 12 shows the comparison of field measurements and simulated values of internal stress of backfill materials and roof subsidence. The red lines denote the simulated stress on the

backfill materials, while green lines indicate the simulated roof subsidence, while the internal stress and roof subsidence of backfill materials obtained through actual measurement are represented by black and blue squares, respectively. With the advance of the backfill panel, the measured values changed consistently with those simulated. This indicated that the model can be used to obtain strata movement and stress distribution characteristics during both the mining and filling processes.

Discussion of simulation results

The curves of surface subsidence and horizontal movement are drawn when the backfill materials with different particle sizes were poured into backfill panels, as displayed in Fig. 13. With increasing particle size, the lower the stiffness of the backfill materials, the larger the deformation, the greater the values of surface subsidence, and the greater the horizontal movement. Figure 13 shows that the maximum values of surface subsidence when employing samples in groups A, B, C, and D were 57.04, 78.61, 80.53, and 58.32 mm, respectively, while those of the horizontal movement were 13.75, 20.02, 20.61, and 14.17 mm, respectively.

Samples in group D had particle sizes ranging from 2.5 to 50 mm with uniform gradation; therefore, slight deformation occurred under the load imposed by the overlying strata. Furthermore, the surface subsidence and horizontal movement when samples in group D were used differed less compared with those of samples in group A, but was less than those when using samples in groups B and C.

Figure 7 shows that the stiffness of samples in group B is significantly superior to that in group C. Nevertheless, few differences were found on the ground surface with regard to its subsidence and horizontal movement. This is

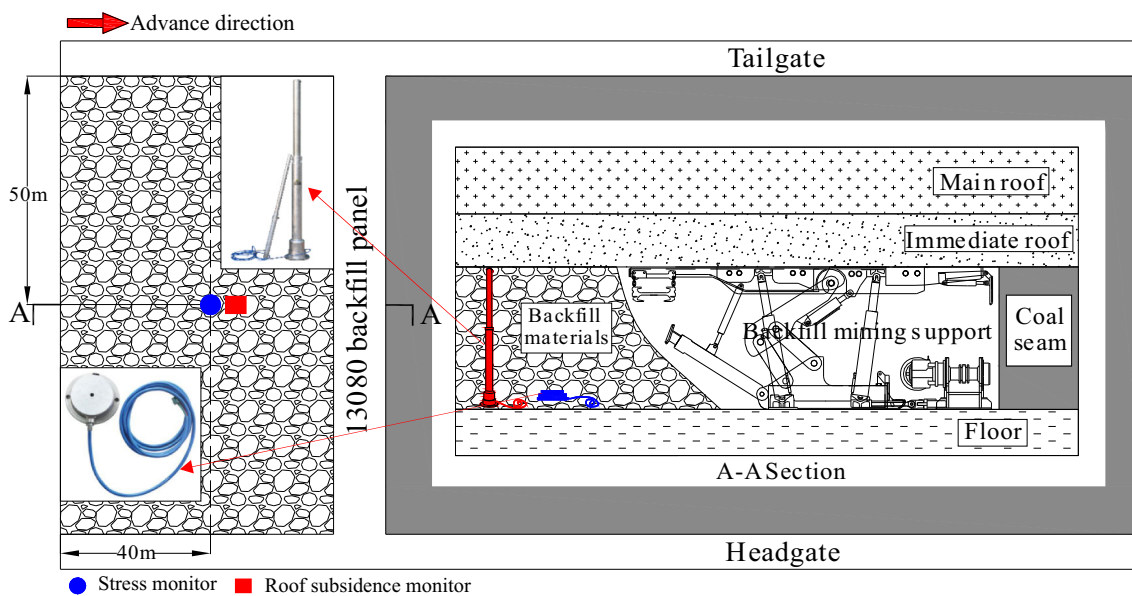


Fig. 11 Field monitoring scheme

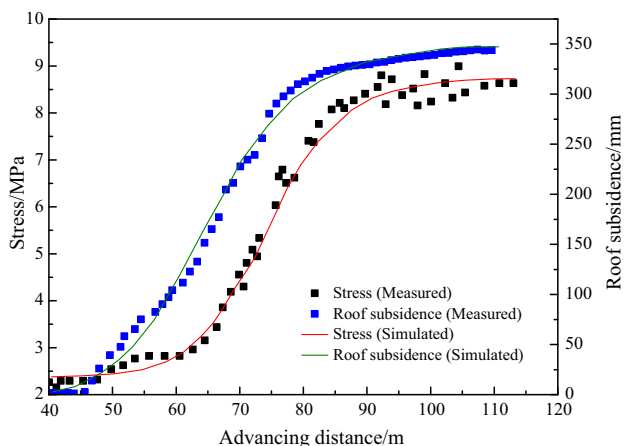


Fig. 12 Comparison of measured and simulated internal stress of backfill materials and roof subsidence

because, after the backfill materials were poured into goafs, the strata did not cave owing to their abilities to resist deformation and the support of backfill materials. Moreover, as the deformation of backfill materials was transferred from the bottom to the top of the strata, the strata prevented some of the deformation in the backfill materials.

The surface inclination, curvature, and horizontal deformation are the main indicators reflecting the characteristics of surface subsidence and movement. Based on the values of surface subsidence and horizontal movement in Fig. 13, the curves of surface inclination, curvature, and horizontal deformation are obtained, as shown in Fig. 14. Table 3 lists the maximum values of surface subsidence and movement.

Figure 14 shows that, in terms of samples in groups A, B, and C, the values of surface inclination, curvature, and horizontal movement increased with the particle size of the CGBM. Moreover, the larger the particle size and porosity, the greater the deformation under the load imposed by the overlying strata, resulting in larger values of surface inclinations, curvature, and horizontal movement. As for samples in group D, owing to their uniform gradation, the particles with larger particle sizes were used as frame structures and those with smaller particle sizes filled the gaps. Consequently, only slight deformation occurred under the load imposed by the overlying strata, and the surface inclination, curvature, and horizontal movement exhibited few differences when samples in group A were used, but were less than those found while applying samples in groups B and C. The maximum surface inclination when using samples in groups A, B, C, and D was 0.165, 0.233, 0.241, and 0.171 mm/m, and the maximum curvatures were 0.00164, 0.00205, 0.00222, and 0.00178 mm/m², respectively. Furthermore, the maximum horizontal deformations were found to be -0.101, -0.145, -0.149, and -0.103 mm/m, respectively. The maximum surface inclination, curvature, and horizontal deformation are less than the destruction extrema of surface buildings on the 13,080 backfill panel.

Due to the mining of coal seams, CGBM are poured into goafs. In this way, the surface subsidence and movement were controlled effectively; thus, the surface buildings were protected. Studying the influence of particle size of CGBM on surface subsidence provides guidance to engineers seeking a better understanding of surface subsidence trends while using this SWBM technique.

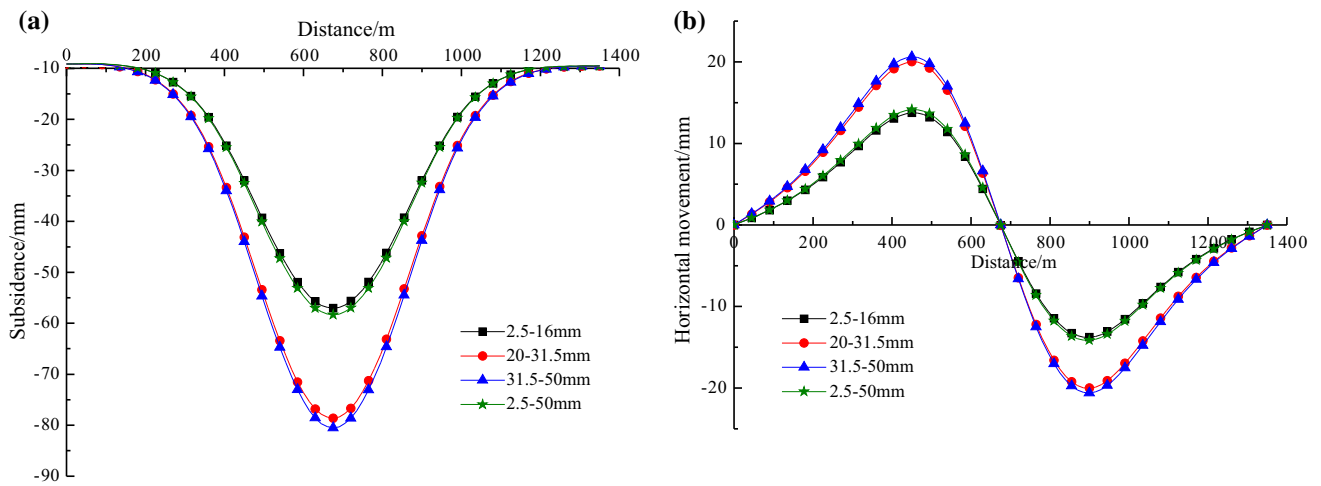


Fig. 13 Surface subsidence and horizontal movement for CGBM with different particle sizes

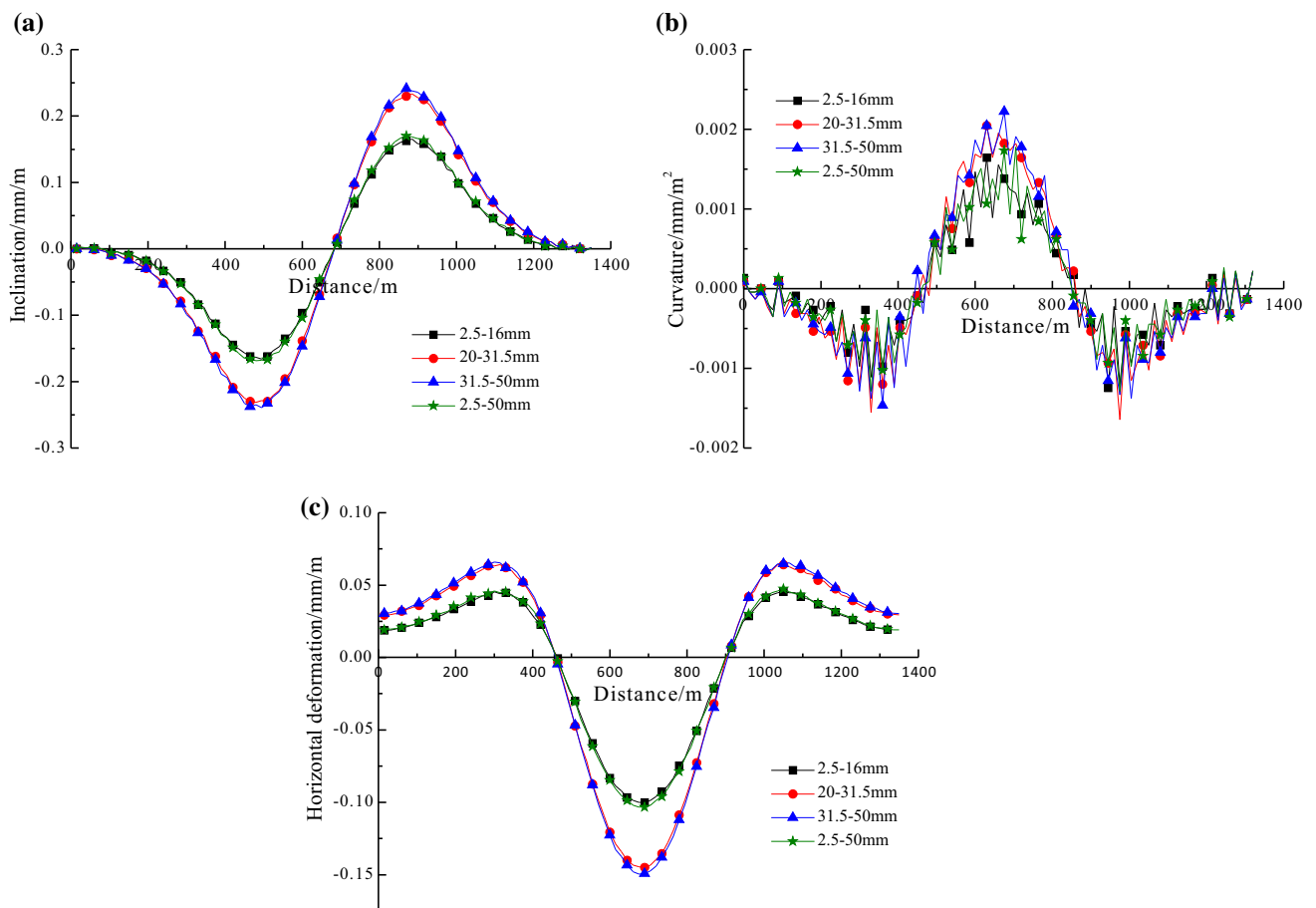


Fig. 14 Inclination, curvature, and horizontal deformation for CGBM with different particle sizes

Conclusions

The SWBM technique uses crushed materials to fill goafs. The particle size of backfill materials is seen as the key factor influencing the controlling effects of surface

subsidence. To analyse the influence of particle size of backfill materials on surface subsidence, this study used a YAS5000 testing machine and a self-made compaction device to test the compaction properties of CGBM with different particle sizes. Furthermore, the stress–strain

Table 3 Maximum surface subsidence and movement after CGBM with different particle sizes were used

Particle size (mm)	Subsidence (mm)	Horizontal movement (mm)	Inclination (mm/m)	Curvature (mm/m ²)	Horizontal deformation (mm/m)
2.5–16	57.04	13.75	0.165	0.00164	−0.101
16–20	78.61	20.02	0.233	0.00205	−0.145
20–31.5	80.53	20.61	0.241	0.00222	−0.149
31.5–50	58.32	14.17	0.171	0.00178	−0.103

curves of CGBM with different particle sizes were obtained and strain hardening of the CGBM was found during compaction. Based on the compaction properties, a method of simulating CGBM using a double-yield model was proposed. By using this method, the authors explored the effect of particle size of CGBM on the surface subsidence. Key results revealed that with an increase in the particle size of the backfill materials, the maximum surface subsidence, horizontal movement, inclination, curvature, and horizontal deformation increased gradually. The surface subsidence and movement after using CGBM with the particle sizes in the range 2.5–50 mm and a uniform gradation show little differences to those when using CGBM with particle sizes in the range 2.5–16 mm. However, the former values were smaller than those obtained after using samples with particle sizes ranging from 20 to 31.5 mm and 31.5–50 mm. This is because the CGBM with a particle size of 2.5–50 mm had a uniform gradation. By using large particles to form frame structures and small particles to fill fractures, the structure was endowed with a high stiffness and underwent only small amounts of deformation under the load imposed by the overlying strata. Therefore, this structure can effectively control the surface deformation.

Acknowledgements This research was supported by the Fundamental Research Funds for the Central Universities (2017XKZD13).

References

Belem T, Benzaazoua M (2008) Design and application of underground mine paste backfill technology. *Geotech Geol Eng* 26:147–174. doi:10.1007/s10706-007-9167-y

Brake SS, Dannelly HK, Connors KA (2001) Controls on the nature and distribution of an alga in coal mine-waste environments and its potential impact on water quality. *Environ Geol* 40:458–469. doi:10.1007/s002540000181

Cui XM, Gao YG, Yuan DB (2014) Sudden surface collapse disasters caused by shallow partial mining in Datong coalfield, China. *Nat Hazards* 74:911–929. doi:10.1007/s11069-014-1221-5

Fan GW, Zhang DS, Wang XF (2014) Reduction and utilization of coal mine waste rock in China: a case study in Tiefsa coalfield. *Resour Conserv Recy* 83:24–33. doi:10.1016/j.resconrec.2013.12.001

Guo GL, Zhu XJ, Zha JF, Wang Q (2014) Subsidence prediction method based on equivalent mining height theory for solid

backfilling mining. *Trans Nonferrous Metal Soc China* 24:3302–3308. doi:10.1016/S1003-6326(14)63470-1

Guo WB, Tan Y, Bai EH (2017) Top coal caving mining technique in thick coal seam beneath the earth dam. *Int J Min Sci Technol* 27:165–170. doi:10.1016/j.ijmst.2016.11.005

Jirina T, Jan S (2010) Reduction of surface subsidence risk by fly ash exploitation as filling material in deep mining areas. *Nat Hazards* 53:251–258. doi:10.1007/s11069-009-9425-9

Junker M, Witthaus H (2013) Progress in the research and application of coal mining with stowing. *Int J Min Sci Technol* 23:7–12. doi:10.1016/j.ijmst.2013.01.002

Li M, Zhang JX, Miao XX (2014) Experimental investigation on compaction properties of solid backfill materials. *Min Technol* 123:193–198. doi:10.1179/1743286314Y.0000000066

Loupasakis C, Angelitsa V, Rozos D, Spanou N (2014) Mining geohazards-land subsidence caused by the dewatering of open-cast coal mines: the case study of the Amyntaio coal mine, Florina, Greece. *Nat Hazards* 70:675–691. doi:10.1007/s11069-013-0837-1

Mohammad N, Reddish DJ, Stace LR (1997) The relation between in situ and laboratory rock properties used in numerical modelling. *Int J Rock Mech Min Sci* 34:289–297. doi:10.1016/S0148-9062(96)00060-5

Oparin VN, Potapov VP, Giniyatullina OL, Andreeva NV, Schastlivtsev EL, Bykov AA (2014) Evaluation of dust pollution of air in Kuzbass coal-mining areas in winter by data of remote earth sensing. *J Min Sci* 50:549–558. doi:10.1134/S1062739114030168

Orejarena L, Fall M (2010) The use of artificial neural networks to predict the effect of sulphate attack on the strength of cemented paste backfill. *Bull Eng Geol Environ* 69:659–670. doi:10.1007/s10064-010-0326-7

Palarski J (1989) The experimental and practical results of applying backfill. In: Hassani FP, Scoble MJ, Yu TR (eds) *Innovations in mining backfill technology*. Balkema, Rotterdam, pp 33–37

Pappas DM, Mark C (1993) Behavior of simulated longwall gob material. Bureau of Mines, Report of Investigations, pp 23–35

Skierszkan EK, Maye KU, Weis D, Beckie RD (2016) Molybdenum and zinc stable isotope variation in mining waste rock drainage and waste rock at the Antamina mine, Peru. *Sci Total Environ* 550:103–113. doi:10.1016/j.scitotenv.2016.01.053

Unver B, Yasitli NE (2006) Modelling of strata movement with a special reference to caving mechanism in thick seam coal mining. *Int J Coal Geol* 66:227–252. doi:10.1016/j.coal.2005.05.008

Wang JA, Shang XC, Ma HT (2008) Investigation of catastrophic ground collapse in Xingtai gypsum mines in China. *Int J Rock Mech Min Sci* 45:1480–1499. doi:10.1016/j.ijrmm.2008.02.012

Xu ZQ (2001) Study of several problems concerning selection of physical and mechanical parameters of rock used for numerical analysis. MS thesis, J Univ Sci Technol B 16–17

Xuan DY, Xu JL (2014) Grout injection into bed separation to control surface subsidence during longwall mining under villages: case study of Liudian coal mine, China. *Nat Hazards* 73:883–906. doi:10.1007/s11069-014-1113-8

- Xuan DY, Xu JL, Wang BL, Teng H (2016) Investigation of fill distribution in post-injected longwall overburden with implications for grout take estimation. *Eng Geol* 206:71–82. doi:[10.1016/j.enggeo.2016.04.007](https://doi.org/10.1016/j.enggeo.2016.04.007)
- Yavuz H (2004) An estimation method for cover pressure re-establishment distance and pressure distribution in the goaf of longwall coal mines. *Int J Rock Mech Min Sci* 41:193–205. doi:[10.1016/S1365-1609\(03\)00082-0](https://doi.org/10.1016/S1365-1609(03)00082-0)
- Zhang JX, Zhou N, Huang YL, Zhang Q (2011) Impact law of the bulk ratio of backfilling body to overlying strata movement in fully mechanized backfilling mining. *J Min Sci* 47:73–84. doi:[10.1134/S1062739147010096](https://doi.org/10.1134/S1062739147010096)
- Zhang JX, Jiang HQ, Deng XJ, Ju F (2014) Prediction of the height of the water-conducting zone above the mined panel in solid backfill mining. *Mine Water Environ* 33:317–326. doi:[10.1007/s10230-014-0310-8](https://doi.org/10.1007/s10230-014-0310-8)
- Zhang JX, Zhang Q, Spearing AJS, Miao XX, Guo S, Sun Q (2017) Green coal mining technique integrating mining-dressing-gas draining-backfilling-mining. *Int J Min Sci Technol* 27:17–27. doi:[10.1016/j.ijmst.2016.11.014](https://doi.org/10.1016/j.ijmst.2016.11.014)